Downloaded from orbit.dtu.dk on: Apr 30, 2024

DTU Library

Cyclic ring fiber textures in single tungsten fiber-reinforced tungsten composites

Ciucani, U. M.; Haus, L.; Gietl, H.; Riesch, J.; Pantleon, W.

Published in:
I O P Conference Series: Materials Science and Engineering

Link to article, DOI:
10.1088/1757-899X/1121/1/012024

Publication date:
2021

Document Version
Publisher's PDF, also known as Version of record

Link back to DTU Orbit

Citation (APA):
Ciucani, U. M., Haus, L., Gietl, H., Riesch, J., & Pantleon, W. (2021). Cyclic ring fiber textures in single tungsten fiber-reinforced tungsten composites. *I O P Conference Series: Materials Science and Engineering*, *1121*(1), Article 012024. https://doi.org/10.1088/1757-899X/1121/1/012024

General rights
Copyright and moral rights for the publications made accessible in the public portal are retained by the authors and/or other copyright owners and it is a condition of accessing publications that users recognise and abide by the legal requirements associated with these rights.

- Users may download and print one copy of any publication from the public portal for the purpose of private study or research.
- You may not further distribute the material or use it for any profit-making activity or commercial gain
- You may freely distribute the URL identifying the publication in the public portal

If you believe that this document breaches copyright please contact us providing details, and we will remove access to the work immediately and investigate your claim.

PAPER • **OPEN ACCESS**

Cyclic ring fiber textures in single tungsten fiber-reinforced tungsten composites

To cite this article: U M Ciucani *et al* 2021 *IOP Conf. Ser.: Mater. Sci. Eng.* **1121** 012024

View the article online for updates and enhancements.

This content was downloaded from IP address 93.163.187.86 on 13/04/2021 at 07:46

Cyclic ring fiber textures in single tungsten fiber-reinforced tungsten composites

U M Ciucani[1], L Haus[1,2], H Gietl[3], J Riesch[3], and W Pantleon[1]

[1] Technical University of Denmark, 2800 Kongens Lyngby, Denmark.
[2] Technical University Freiberg, 09599 Freiberg, Germany.
[3] Max-Planck-Institute for Plasma Physics, 85748 Garching, Germany.

Email: pawo@dtu.dk

Abstract. Tungsten fiber-reinforced tungsten composites are considered as plasma-facing material in future fusion reactors. Such composites are obtained by chemical vapor deposition of tungsten on potassium-doped, drawn tungsten wires. In model composites containing single fibers, particular texture types develop due to the cylindrical geometry of the deposition process. The vapor-deposited tungsten layers form a cyclic <100> ring fiber texture with one of the <100> directions pointing radially along the growth direction. The procedure for revealing this non-standard texture type from orientation data obtained by electron backscatter diffraction is presented. Identification of cyclic textures requires carefully chosen acquisition regions as well as a suitable coordinate system for their analysis. It is demonstrated that quite erroneous conclusions about the texture of the layer would be drawn if this is not accounted for properly.

1. Introduction

Tungsten is considered for plasma-facing components in future fusion reactors as armor material for the first wall and the divertor. In particular, tungsten fiber-reinforced tungsten composites have achieved certain interest due to their pseudo-ductile behavior [1]. Such composites can be obtained by chemical vapor deposition of tungsten on drawn tungsten wires [2]. The microstructure of a model composite containing a single potassium-doped tungsten fiber is investigated by means of electron backscatter diffraction [3]. Focus is on revealing the particular texture caused by deposition geometry.

2. Materials and techniques

2.1. Material

A tungsten fiber-reinforced tungsten composite is produced by chemical vapor deposition of tungsten on a single tungsten fiber: A drawn tungsten wire doped with 60 ppm potassium and having a diameter of 150 µm provided by OSRAM GmbH is coated in a two-step process by reactive magnetron sputtering with a 1 µm thin interlayer of erbia. A thick layer of pure tungsten (referred to as matrix) is chemically vapor-deposited on this interlayer to a total diameter of 1.5±0.1 mm (for details see [3]). Figure 1 sketches the geometry of the cylindrical specimen. A cross section is cut perpendicular to the cylinder axis, i.e. the wire axis, and prepared for electron backscatter diffraction by mechanical grinding (on SiC-paper of grit size 2000 and 4000) and polishing (with diamond suspension with grain size 3 µm). In a final step, electro-polishing is applied using an aqueous solution containing 3 wt.% NaOH at room temperature with an applied voltage of 12 V and a current of approximately 2 A.

Content from this work may be used under the terms of the Creative Commons Attribution 3.0 licence. Any further distribution of this work must maintain attribution to the author(s) and the title of the work, journal citation and DOI.
Published under licence by IOP Publishing Ltd

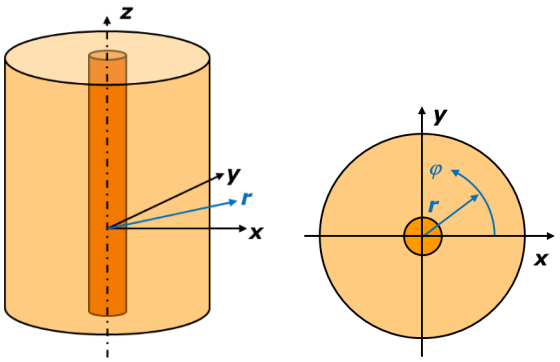

Figure 1. Sketch of the geometry of a cylindrical single tungsten fiber-reinforced tungsten composite (left) and its cross section (right). Upon a drawn, potassium-doped tungsten wire (shown in dark orange) coated with a thin erbia layer (not shown), tungsten is chemically vapor-deposited (light orange). Additional to the Cartesian coordinate system (black), a cylindrical coordinate system is introduced (blue). The radial direction r points in a transversal xy-plane outwards from the wire center, the azimuthal direction φ along the perimeter.

2.2. Microstructural investigation

Orientation data were gathered by electron backscatter diffraction on freshly prepared cross sections using a Bruker NOVA NanoSEM 600 equipped with a Bruker e-Flash HD EBSD detector applying a voltage of 20 kV. A large overview map 2000x1725 µm^2 of the entire cross section is recorded at low magnification with a step size of 5 µm. Without any filtering or removal of non-indexed points, the gathered electron backscatter diffraction data are analyzed using the MTEX toolbox Version 5.5.0 [4] and evaluated further by own purposely developed routines.

3. Results

3.1. Conventional analysis

Figure 2 presents the obtained orientation maps colored according to the crystallographic direction along the three different directions of a Cartesian coordinate system: the z-direction is normal to the mapped surface, the x- and y-direction correspond to the horizontal and vertical direction in the map, respectively. The cylindrical specimen can be recognized by the indexed points surrounded by a white, non-indexed region in the rectangular map. A clearly discernible central region of non-indexed points with diameter of 150 µm marks the locations of the drawn wire and the erbia interlayer. Due to defects formed by the large plastic deformation during wire drawing, orientations within the wire cannot be resolved with the chosen acquisition conditions for obtaining a large overview map. The successfully acquired orientations belong overwhelmingly to the chemically vapor-deposited tungsten matrix.

The orientation maps in figure 2 also highlight high angle boundaries which together with the orientation coloring reveal that in the vicinity of the wire a large number of small grains prevail which are not even resolved properly. In slightly larger distances from the wire, large grains are observed which stretch radially from the vicinity of the wire to the outer surface. These matrix grains grow radially and their wedge-like shape is a signature of the deposition process. The orientation map in figure 2c highlighting the crystallographic directions along the z-direction show dominantly colors from red over yellow to green, i.e. along the line [100]-[110], whereas bluish colors (blue, cyan or magenta) are rarely observed. This indicates the presence of preferred orientations. Further details about the texture are revealed from the corresponding pole figures in figure 3, displaying the crystallographic poles as a function of the spatial directions. The pole figures are derived based on the orientation distribution function calculated from all individual orientations in the map using a de la Valle Poussin kernel [4] with a half width of 10°.

Figure 3a presents the pole figures for the 100, 110 and 111 poles in stereographic projection onto the xy-plane. A maximum pole density of 2.6 compared to a random distribution of orientations is observed in the 100 pole figure where also an increased pole density along the outer perimeter is noticed. Judging solely from this 100 pole figure, the existence of a weak <100> fiber texture along the cylinder axis would be concluded. Further support for an ideal <100> fiber texture is gained from the very weak ring at 45° in the 110 pole figure, but the apparent ring in the 111 pole figure at about 36° contradicts the idea entirely, as such a ring is expected at 54° for an ideal <100> fiber texture.

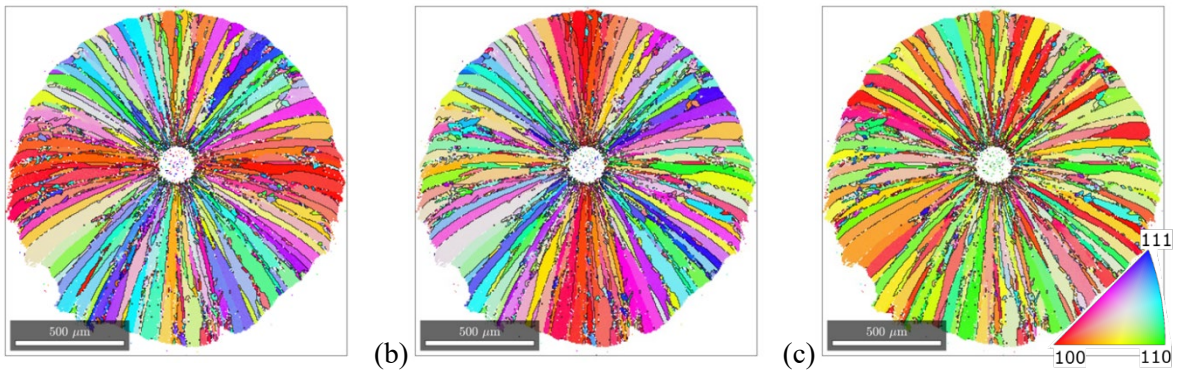

(a) (b) (c)

Figure 2. Orientation maps of the cross section of a single tungsten fiber-reinforced tungsten composite with erbia interlayer. The colors reflect the crystallographic directions along different sample directions according to the inset: (a) along *x*-, (b) along *y*- and (c) along *z*-direction, i.e. along the wire axis. High angle boundaries with disorientation angles above 15° are indicated in black.

These observations are confirmed by the inverse pole figure in figure 3b along the *z*-axis which indeed shows a slight preference of [100] directions, but all directions along the symmetry line [100]-[110] are much more frequent than expected for an ideal <100> fiber texture along the *z*-direction.

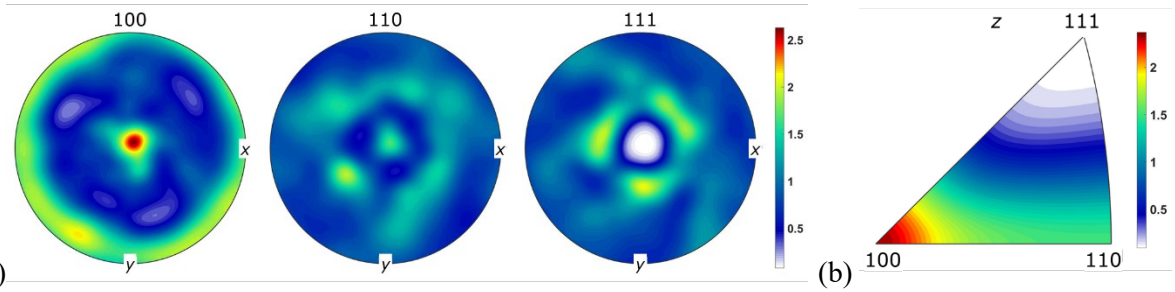

(a) (b)

Figure 3. (a) 100, 110, and 111 pole figures and (b) inverse pole figure for *z*-direction obtained on a single tungsten fiber-reinforced tungsten composite with erbia interlayer. The data include all acquired orientations from the cross section shown in figure 2 and correspond overwhelmingly to locations in the matrix. All densities are given in multiples of random distribution according to the scale bar.

3.2. Improved analysis

In view of this evidence, the texture of the matrix cannot be a <100> fiber texture with a fiber axis along the wire and a more appropriate description of the texture is required. Revisiting the orientation maps in figure 2 exposes a hint: in figure 2a showing the crystallographic direction along the *x*-direction, the color red is dominating along a horizontal stripe in the center of the cross section revealing that horizontally aligned grains extend along one of their <100> directions. A similar observation can be made from figure 2b showing the crystallographic direction along the *y*-direction; here the red color of vertically aligned grains indicates that these also extend along one of their <100> directions, which in their case points along the *y*-direction, i.e. vertically instead of horizontally. Considering the cylindrical symmetry of the specimen, it seems plausible to conclude that all grains actually extend along one of their <100> directions radially outwards.

In order to exploit the observation that the grains exhibit a particular direction of extension along which one of their <100> directions is aligned, but that this direction is different from grain to grain, a special procedure for analyzing the texture is adapted. In view of the geometry of the specimen and the deposition process, a cylindrical coordinate system is introduced as shown in figure 1 where the radial *r*-direction points radially outwards from the wire center and the azimuthal φ-direction along the corresponding perimeter (the *z*-axis still coincides with the wire axis). In such a cylindrical coordinate system, the coordinate axes *r* and φ point in different directions at each position in a transversal plane.

For calculating pole figures and inverse pole figures with respect to these new coordinate axes, their local dependence must be taken into account. Such an evaluation is presently not implemented in any standard tool for evaluating orientation data. An appropriate procedure has been developed and implemented in MATLAB. The idea is basically to use standard evaluation tools for creating orientation maps, pole figures and inverse pole figures – not on the original orientations, but after a straightforward modification of the orientations in the map: Realizing that the cylindrical coordinate system is rotated by the azimuthal angle φ with respect to the Cartesian system at any position in the map, the Euler angle φ_2 of each orientation is adjusted accordingly. The resulting orientation maps, pole figures and inverse pole figures are on display on figures 4 and 5.

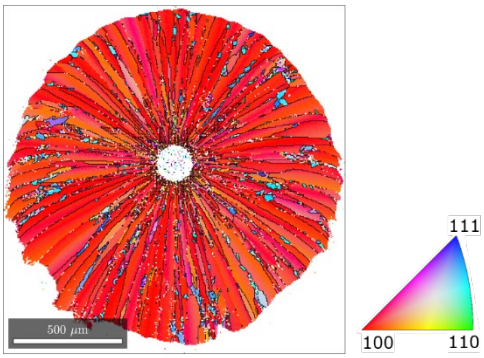

Figure 4. Orientation map of the cross section of a single tungsten fiber-reinforced tungsten composite with erbia interlayer (same data as in figure 2). The colors reflect the crystallographic directions along the radial direction of a cylindrical coordinate system according to the inset. High angle boundaries with disorientation angles above 15° are indicated in black.

In the orientation map in figure 4 colored according to the crystallographic direction along the radial direction, a dominating red color appears exposing an overwhelming dominance of <100> directions pointing radially outwards. The character of the texture is further confirmed by the pole figures in figure 5a. In the 100 pole figure, a strong alignment of crystallographic <100> directions with the radial direction is seen (with a maximum 100 pole density of 10.5), the ring in the plane comprising the azimuthal and axial direction is a direct consequence of this strong alignment and the angle of 90° between <100> directions. In a similar way, <110> directions form either an angle of 45° or 90° degrees with <100> explaining neatly the observed rings in the 110 pole figure. Finally, the angle of 54° between <111> and <100> directions rationalizes the position of the rings in the 111 pole figure. All rings in the pole figures are rather smoothly populated and no systematic variation is observed along them indicating the presence of an ideal <100> fiber texture along the radial direction.

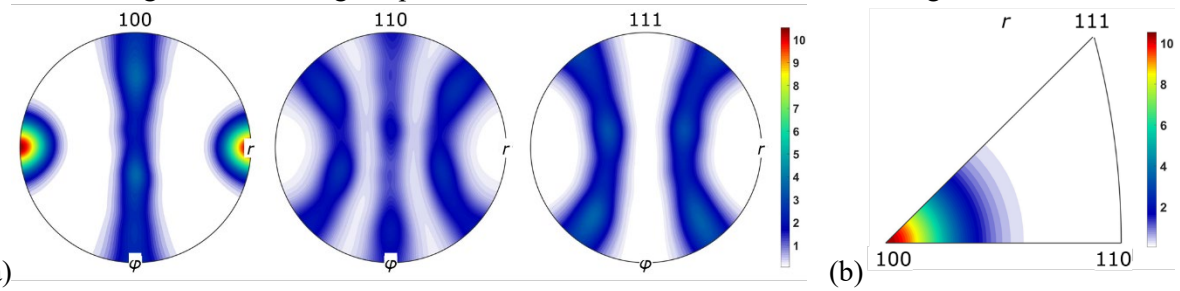

Figure 5. (a) 100, 110, and 111 pole figures with respect to cylindrical coordinates and (b) inverse pole figure along the radial *r*-direction obtained on a single tungsten fiber-reinforced tungsten composite with erbia interlayer. The data include all acquired orientations from the cross section shown in figure 2 and correspond overwhelmingly to locations in the matrix. The densities are given in multiples of random distribution according to the scale bar.

In consequence, the texture is a strong, ideal <100> fiber texture along the radial direction in the cylindrical coordinate system and not a weak <100> fiber texture along the axial direction as may have been concluded from investigating the texture in a Cartesian coordinate system. In view of these findings, the texture in the sample system must be described differently: At first, there is a preferred alignment of <100> directions in the transversal plane with free rotation around that aligned direction.

Such textures are classified as ring fiber textures [5] (alternatively, the term planar texture is used [6]). Additionally to one of the <100> directions occurring in the transversal plane (and free rotations around it), this specific direction aligns with the radial direction causing a different preferred orientation at any spatial position. Textures featuring a certain crystallographic direction aligned with the radial direction are termed cyclic textures [5,7] (or cylindrical textures [8] or circular textures [9]) and usually discussed in connection with cylindrical objects (wires or tubes). In consequence, the texture of the deposited layer must be classified as cyclic <100> ring fiber texture.

4. Discussion

A cyclic <100> ring fiber texture is concluded for the deposited layer with <100> directions aligned in the transversal plane perpendicular to the wire axis and the particular feature from cylindrical symmetry, that these <100> directions point radially. The possibility of cyclic ring fiber textures has been discussed theoretically [5], but to the knowledge of the authors never been reported before.

Cyclic fiber textures and cyclic ring fiber textures might be more widespread than commonly reported, because it might be difficult to resolve spatial correlations between preferred orientations as in the present case. To illustrate the danger of underestimating the impact of spatial correlations for obtaining a proper texture description, different regions of the original map are analyzed separately. Four different subsets of orientations are obtained from four smaller quadratic or rectangular regions (each comprising about half the number of indexed points) as illustrated in the top row of figure 6.

The corresponding 100 pole figures in the bottom row of figure 6 show rather different pole distributions: From the 100 pole figure of the entire map (figure 6a), a <100> fiber texture along the *z*-axis would be concluded naively. For the square region in figure 6b, 100 poles are observed under 45° with respect to *x*- and *y*-direction implying preferred orientations belonging to a {100}<011> texture component (a cube orientation rotated by 45° around *z*); for the rotated square region (figure 6c), 100 poles along both *x*- and *y*-direction are dominating implying the presence of an ideal {100}<001> cube component; for the horizontal rectangle, 100 poles appear along the *x*-direction and an additional ring in the *yz*-plane (in figure 6d) implying a <100> fiber texture along the *x*-axis. Just the opposite is true for the vertical rectangle; the 100 pole figure in figure 6e indicates a <100> fiber texture along the *y*-direction. Hence, depending on the choice of the region from which orientations are acquired, rather different texture types are concluded based on the 100 pole figures as summarized in table 1: in some cases, fiber textures with different fiber axes (<100> fiber texture along *x*-, *y*-, or *z*-direction), in other cases, textures with orthorhombic symmetry (cube or rotated cube).

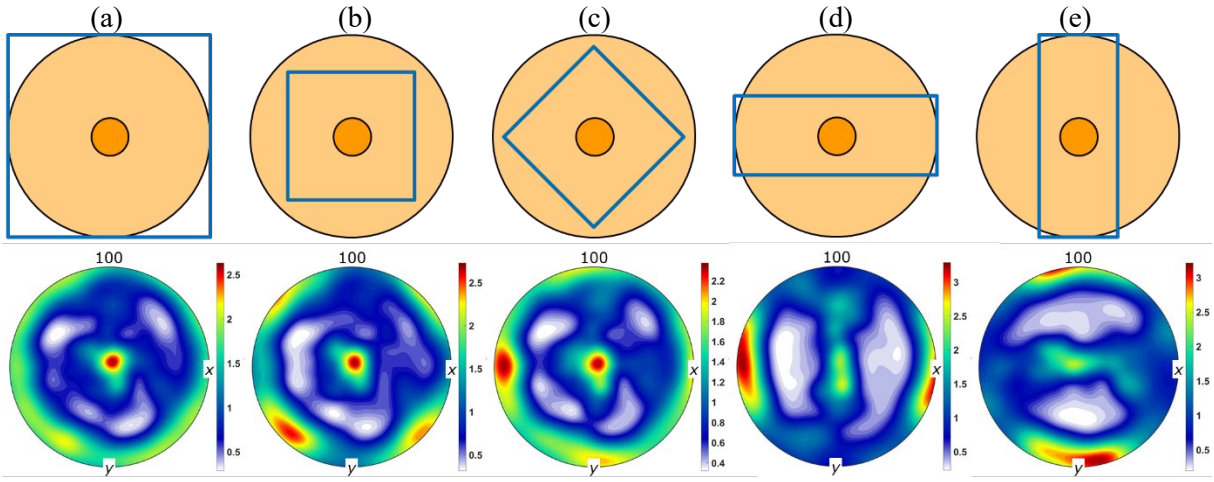

Figure 6. Schematic drawing of different acquisition regions on the cross section of a single tungsten fiber-reinforced tungsten composite with erbia interlayer (top row) and corresponding 100 pole figures (bottom row) for (a) data acquired for the entire cross section corresponding to figure 2, (b) to (e) different square and rectangular regions with about half of the number of indexed points.

Table 1. Quantitative texture analysis for different regions on the cross section (cf. figure 6)

Region	Max. 100 pole density	Texture index	Texture entropy	Texture type (as concluded from 100 pole figure)
Full map (Cartesian coord.)	2.6	1.55	-0.28	<100> fiber texture along *z*
Full map (cylindrical coord.)	*10.5*	*5.09*	*-1.16*	*Cyclic <100> ring fiber texture*
Central square	2.7	1.62	-0.29	{100}<011> *z*-rotated cube texture
Rotated square	2.4	1.51	-0.26	{100}<001> cube texture)
Horizontal rectangle	3.3	1.92	-0.39	<100> fiber texture along *x*
Vertical rectangle	3.2	1.84	-0.38	<100> fiber texture along *y*

The cyclic nature of the texture can be substantiated further by the measures of texture strength in table 1: When using a Cartesian coordinate system, independent of the chosen region rather weak textures are indicated by 100 pole densities of maximal 3.3, texture indices [10] less than 2 and texture entropies [11] above -0.4. Using an appropriate cylindrical coordinate system with spatially different coordinate axes for the description of the orientations confirms the strong preference of certain directions and orientations seen in the pole figures and inverse pole figure in figure 4. The maximal 100 pole density of 10.5 verifies that a much better texture description is achieved by realizing the presence of a cyclic texture. The existence of a strong cyclic ring fiber texture is further substantiated by the high texture index above 5 and the large negative value -1.16 of the texture entropy.

5. Conclusion

A tungsten fiber-reinforced tungsten composite has been investigated by electron backscatter diffraction. The chemically vapor-deposited tungsten matrix shows a peculiar texture identified as cyclic <100> ring fiber texture. The required thorough texture analysis is detailed and the effect of inappropriate choices for the acquisition regions outlined. This clearly demonstrates how important an adequate characterization becomes and how strongly results can be affected by spatial correlations, if sample symmetry is not respected. When using an inappropriate coordinate system, completely erroneous textures might be concluded. On the other hand, when utilizing an appropriate coordinate system even more complicated texture types can be identified as the cyclic <100> ring fiber texture.

Acknowledgments

This work has been carried out partially within the framework of the EUROfusion Consortium and has received funding from the Euratom research and training programme 2014-2018 and 2019-2020 under grant agreement No 633053. The views and opinions expressed herein do not necessarily reflect those of the European Commission.

References

[1] Riesch J, Höschen T, Linsmeier C, Wurster S, and You J H 2014 *Phys. Scr.* **2014** 014031
[2] Du J, You J H, and Höschen T 2012 *J. Mater. Sci.* **47** 4706
[3] Ciucani U M, Haus L, Gietl, H, Riesch J, and Pantleon W 2021 *J. Nucl. Mater.* **543** 152579
[4] Bachmann F, Hielscher R, and Schaeben H 2010 *Solid State Phenom.* **160** 63
[5] Wassermann G and Grewen J 1962 *Texturen metallischer Werkstoffe* 2nd edition (Berlin: Springer Verlag) pp 7-11
[6] Saraf R F 1994 *Polymer* **35** 1359
[7] Stüwe P 1961 *Z. Metallkde.* **52** 34
[8] Leber S 1961 *Trans. Amer. Soc. Metals* **52** 697
[9] Kocks U F, Tomé C N, and Wenk H.-R. 1998 *Texture and Anisotropy* (Cambridge: Cambridge University Press) p 151
[10] Bunge H.-J. 1982 *Texture Analysis in Materials Science* (Butterworth & Co) p 88
[11] Schaeben H 1988 *J. Appl. Phys.* **64** 2236